Biochemical Pharmacology 78 (2009) 1316–1322

Contents lists available at ScienceDirect

Biochemical Pharmacology

journal homepage: www.elsevier.com/locate/biochempharm

Tanshinone IIA triggers p53 responses and apoptosis by RNA polymerase II upon DNA minor groove binding

Zhichao Zhang [a,*], Jin Gao [b], Yuanyuan Wang [c], Ting Song [b,d], Jing Zhang [b], Guiye Wu [a], Tiantai Zhang [e,**], Guanhua Du [e]

[a] State Key Laboratory of Fine Chemicals, Dalian University of Technology, Dalian 116012, PR China
[b] School of Environmental and Biological Science and Technology, Dalian University of Technology, Dalian 116024, PR China
[c] Genetic Engineering Division, Xinao Research Institute, Langfang, PR China
[d] State Key Laboratory of Natural and Biomimetic Drugs, Peking University, Beijing 100191, PR China
[e] National Center for Drug Screening, Institute of Materia Medica, Chinese Academy of Medical Sciences & Peking Union Medical College, Beijing 100050, PR China

ARTICLE INFO

Article history:
Received 9 April 2009
Accepted 29 June 2009

Keywords:
Tanshinone IIA
DNA minor groove binder
RNA polymerase II
Apoptosis

ABSTRACT

Our previous work has shown that tanshinone IIA (Tan IIA) is a DNA minor groove binder instead of an intercalator as previously thought. In this study, we have further demonstrated that the molecular antitumor pharmacology of Tan IIA is dependent on its groove-binding capability. First, we investigated the structure damage to duplex DNA upon Tan IIA binding using circular dichroism spectra. Subsequently, we performed western blot, flow cytometry analysis, chromatin immunoprecipitation, and quantitative real-time PCR to illustrate the RNAPII degradation, phosphorylation, and distribution along the transcribed gene in H22 cells exposed to Tan IIA. In addition, p53 activation and apoptosis induction in both cultured H22 cells and in mice bearing the ascitic-type H22 were measured following Tan IIA treatment. It was revealed that Tan IIA decreases the level of RNAPII by altering DNA structure. At the low dose range (0.2–4 μM) of Tan IIA exposure, the DNA structure damage results in the inhibition of RNAPII binding to DNA and the initiation of RNAPII phosphorylation, while higher concentrations of Tan IIA (4–20 μM) cause complete phosphorylation and degradation of RNAPII followed by p53 activation and apoptosis. A similar apoptosis induction by RNAPII was observed in animals. Apoptosis of tumor cells from ascitic fluid was not detected until RNAPII levels were downregulated by Tan IIA, which requires 40 mg/kg body weight of Tan IIA. It was concluded that DNA-conformational-damage-dependent RNAPII response upon groove binding is the molecular basis of the antitumor property of Tan IIA, *in vivo* and *in vitro*.

1. Introduction

Tanshen (*Salvia miltiorrhiza* bunge) has been widely used in traditional Chinese medicine (TCM) practice for thousands of years in the treatment of multiple diseases such as coronary heart diseases, hemorrhage, dysmenorrheal, miscarriage, swelling, insomnia, and inflammatory diseases. As the aged-related diseases developing, the antitumor property of Tanshen attracted more and more interests [1]. As one of the most abundant extracts of Tanshen, Tan IIA has been found to effectively activate the tumor suppressor protein p53 and induce apoptosis [2]. The widely accepted hypothesis of the cytotoxicity of Tanshiones is that they could damage DNA by intercalation due to the planar phenanthrene ring, and free radicals generated by the furano-*o*-quine moiety [3]. Although the hypothesis is so primary that no experimental result may support it, it was cited by almost all the reports on Tan IIA to explain its cytotoxicity. But there is an obvious conflict between this structure-based cytotoxicity and the wide and safe use of Tanshen for numerous diseases other than tumor for thousands of years. Additionally, the hypothesis could only explain a part of the findings in structure–activity-relationship study (SAR) of Tanshinones' cytotoxicity [4]. Thus, we began the investigation to unveil the exact molecular basis for the cytotoxicity of Tan IIA and discussed under which conditions it may exhibit cytotoxicity.

Our recent work has completely denied the aforementioned hypothesis [5]. It was shown that Tan IIA interacts with DNA by minor groove binding preferentially to AT-rich sequences of duplex DNA in stead of intercalation, and no free radical-mediated DNA damage is found in living cells after Tan IIA treatment. Furthermore, all of the findings in SAR study of Tanshinones could

* Corresponding author at: No. 158-89, Zhongshan Road, Dalian 116012, PR China. Tel.: +86 411 39893872; fax: +86 411 83673488.
** Corresponding author at: No. 1, Xian Nong Tan Street, Xuan Wu District, Beijing 100050, PR. China. Tel.: +86 10 63165227; fax: +86 10 63165227.
E-mail addresses: zczhang@dlut.edu.cn (Z. Zhang), ttzhang@imm.ac.cn (T. Zhang).

0006-2952/$ – see front matter © 2009 Elsevier Inc. All rights reserved.
doi:10.1016/j.bcp.2009.06.110

be explained easily according to the groove-binding mode [4,5]. A new hypothesis about the antitumor molecular pharmacology of Tan IIA was raised that the DNA conformational change upon groove binding contributes to Tan IIA's antitumor property.

Many groove binders used as clinical antitumor drugs act by altering duplex DNA structure and therefore may interfere with transcription by RNA polymerase II (RNAPII) [6]. Distamycin A, for example, could destabilize the preinitiation complex and arrest transcription by altering the conformation of DNA [7]. In the similar way, other minor-groove-binding drugs DAPI and mithramycin also block transcription by RNAPII [8].

Since Tan IIA also exhibits minor groove-binding property, we investigated in this study whether or not the transcription mechanism is involved in its antitumor pharmacology. For the first time, it was revealed that Tan IIA induces p53 mediated apoptosis by RNAPII upon groove binding.

2. Materials and methods

2.1. Chemicals and reagents

Tan IIA and cryptotanshinone (chemical correspondent product) were purchased from Shanghai Shunbo Bioengineering Co. (Shanghai, China). The purity is over 98% according to HPLC analysis. Distamysin A was purchased from Sigma–Aldrich Co. (USA). Tris base was from Promega Co. (USA). Calf thymus DNA (CT DNA) was obtained from Sigma–Aldrich Co. (USA).

Stock of CT DNA was prepared by dissolving commercial nucleic acid in Tris–HCl buffer (pH 7.0). The concentration of CT DNA was determined spectrophotometrically using the molar absorption coefficients of $\varepsilon_{260\ nm} = 6600\ M^{-1}\ cm^{-1}$, $\varepsilon_{254\ nm} = 8400\ M^{-1}\ cm^{-1}$ and $\varepsilon_{258\ nm} = 6600\ M^{-1}\ cm^{-1}$, respectively. Doubly purified water used in all experiment was from MILLI-Q system.

2.2. Cells and chemicals treatment

Hydroperitoneum hepatoma cells (H22 cell line) and erythromegakaryoblastic leukemia cells (K562 cell line) were routinely cultured in RPMI 1640 medium with 10% (v/v) fetal calf serum, respectively. Tan IIA was dissolved in DMSO (4 mM) and subsequently stored as stock solutions in dark-colored bottles at 4 °C. The stock was diluted to the required concentration immediately before addition to the growth media. Exponentially growing cells were exposed to various concentrations of Tan IIA for the indicated periods of time. Cells that were grown in media containing an equivalent amount of DMSO without any chemical served as a control.

2.3. Animals

Mice bearing the ascitic-type hepatocarcinoma H22 were purchased from the Institute of Materia Medica, Chinese Academy of Medical Sciences (Beijing, China). Healthy BALB/c mice (CLA grade, 10 weeks, weight 34–36 g) were obtained from Dalian Laboratory Animal Center (Dalian, China) and were bred there. All experiments were performed according to institutional ethical guidelines on animal care approved by Dalian University of Medical Science.

2.4. Circular dichroism spectra

Circular dichroism (CD) spectra were scanned with a J-810 spectrophotometer (Jasco, Japan), using a 1-cm path quartz cell and subtracted from the spectrum of buffer alone. The optical chamber of the CD spectrometer was deoxygenated with dry nitrogen before use and kept in a nitrogen atmosphere during experiments. Scans were accumulated twice and automatically averaged. The intrinsic circular dichroism spectra in 235–305 nm were recorded with a scanning speed of 200 nm min^{-1}. All the CD titrations were done by keeping a fixed DNA concentration at 100 μM and varying the compound concentration from 0 to 40 μM.

2.5. Western blot and antibodies

After cells were exposed to Tan IIA at various concentrations, they were lysed in a lysis buffer (62.5 mM Tris–HCl, pH 6.8, 2% (w/v) SDS, 10% glycerol, 50 mM DTT, 1 mM PMSF). Whole cell lysates equivalent to 100 μg of protein were separated by 6% SDS-PAGE. After electrophoresis, the proteins were transferred to a PVDF membrane (Millipore, Bedford, MA). The membranes were subsequently blocked with a blocking solution containing 5% nonfat dry milk in TBS-T for 1 h at room temperature and were then incubated with each antibody for 1 h at room temperature. The membranes were also incubated with a peroxidase-conjugated IgG, and the expected proteins were detected using the ECL method. Antibodies used include: A-10 Ab against RNAPII (sc-17798, Santa Cruz Biotechnology, USA); H5 Ab against RNAPII CTD phosphorylated on Ser2 (MMS-129R, Covance, USA); DO-1 Ab against p53 (sc-126, Santa Cruz Biotechnology, USA); C4 Ab against β-actin (sc-47778, Santa Cruz Biotechnology, USA); and anti-mouse or anti-rabbit IgG antibody conjugated to horseradish peroxidase (Santa Cruz Biotechnology, USA).

2.6. Chromatin-immunoprecipitation (ChIP) procedures

Chromatin preparation and ChIP procedures have been described previously [9]. Briefly, after treatment with different concentrations of Tan IIA for 48 h, cells were fixed with 1% (v/v) formaldehyde for 15 min at room temperature, and the chromatin was sonicated to an average DNA fragment size of 300–400 bp. The chromatin was equilibrated in RIPA buffer and samples were pre-cleared with non-immune rabbit serum. Equal amounts of pre-cleared chromatin were then incubated with the specific antibody or non-immune IgG in order to measure background recoveries. The immunoprecipitated DNA was purified after proteinase K treatment and phenol extraction. The DNA recovery was measured using a SYBR Q-PCR (SYBR Premix Ex Taq kit for Real Time, TaKaRa, Dalian, China) with a Smart Cycler II (TaKaRa, USA). The PCR was performed in a final volume of 25 μL containing primers (0.5 μM) and amplified using the following conditions: a step at 95 °C for 10 s followed by a step composed of a 5 s period at 95 °C and a 20 s period at 60 °C for a total of 45 cycles. The primers to amplify the fragment A (P2 promotor) gene were 5′-GAGAAGGGCAGGGCTTCTCA-3′ (sense) and 5′-TCTGCCTCTCGCTGGAATTA-3′ (antisense). The primers to amplify the fragment B (exon fragment) gene were 5′-CCTCTGTT-GAAATGGGTCTGG-3′ (sense) and 5′-CCTTTGCCTACCTCTCACCT-TCT-3′ (antisense). The primers to amplify the C fragment (intron fragment) were 5′-TCCACCTCCAGCTTGTACCTG-3′ (sense) and 5′-TCGTTGAGAGGGTAGGGGAAG-3′ (antisense). These experiments were repeated in triplicate. The specificity of the PCR products was routinely controlled by performing melting curve analyses and analyzing via agarose gel electrophoresis. In addition, several criteria were followed in order to verify that each measurement and the recovered DNA were normalized relative to the maximal recovery.

2.7. Fluorescence imaging

H22 cells were cultured as above. 24 h after 8 μM Tan IIA and cryptotanshinone exposure, respectively, the cells were harvested and stained by LIVE/DEAD/APOPTOSIS detection kit according to the protocol provided with the kit (Keygen Biotech. Co. Ltd., China). Fluorescence microscopy images were taken by a Nikon

fluorescence microscope (TE2000, Japan) equipped with a real-time video camera and a standard fluorescence excitation filter set. For every sample, apoptotic cells or dead cells were counted in at least 50 randomly selected, noncontiguous, 200× microscopic fields.

2.8. Flow cytometry analysis

For the expression assays of p53, H22 cells exposed to different concentrations of Tan IIA for 24 h, were harvested, treated with trypsin (0.1% trypsin in PBS for 5 min), fixed in 1 mL of 95% ethanol, and kept at room temperature for 20 min before analysis of antibody binding. Antibody staining was performed as described previously [10]. Briefly, 5×10^5 cells were centrifuged and resuspended in p53 antibody. After 1 h, cells were rinsed and resuspended in a medium containing a secondary antibody conjugated with FITC. The cell pellets were finally resuspended in PBS. The fluorescence of 10,000 cells was analyzed using a FACScan flow cytometer in combination with CellQuest software (BD Biosciences, San Jose, CA). All of the experiments were repeated at least three times.

For the apoptosis assays, hypodiploid DNA was measured as described previously [11]. Briefly, cells were seeded into 6-well plates and treated with drug vehicle (0.1% DMSO) alone or different concentrations of Tan IIA (2.5, 4, 10, and 20 μM, respectively) for 48 h. Subsequently, 10^6 cells were centrifuged and fixed in 1 mL of ice-cold 70% ethanol for 12 h, washed once with PBS, and resuspended in 1 mL of PBS containing 0.04 mg of RNase A and 0.05 mg of propidium iodide. After incubation at room temperature for 30 min the cells were analyzed. The fluorescence from 30,000 cells was counted for each sample. The results were analyzed using a FACScan flow cytometer in combination with CellQuest software.

2.9. Administration of ascitic-type hepatic carcinoma H22 mice model

The mouse bearing the ascitic-type hepatocarcinoma was sacrificed 6–8 days after tumor implant. The ascitic fluid was drawn through the abdominal cavity using a sterile syringe, and then diluted to a concentration of 1×10^7 cells per mL in PBS. 0.2 mL of diluted solution was injected into the abdominal cavity of each BALB/c mouse. After 5 days of inoculation, animals were randomly divided into three groups of 10 mice each. Tan IIA was dissolved in 0.5% CMC prior to use. The control group was given 0.5% CMC (i.p.), while other two groups received i.p. injection every other day with various concentrations of Tan IIA for 10 days (20 and 40 mg/kg body weight, respectively). The design of the dosage was based on the previous reports [2,12].

2.10. Terminal deoxynucleotidyl transferase-mediated dUTP nick end labeling (TUNEL) method

After administered with Tan IIA for 10 days, the ascitic fluid was obtained. The ascitic tumor cells were harvested by centrifugation. The TUNEL method [13] was used according to the manufacture's instructions (Roche, Switzerland) to determine the frequency of apoptosis within tumor cells.

2.11. Statistical analysis

Mean and standard deviation (S.D.) were calculated for each parameter. Results were expressed as mean ± S.D. Comparisons of each group were evaluated by one-way analysis of variance (ANOVA). When the twice of S.D. was higher than the mean, non-parameter test was used to evaluate the difference. A significant difference was assumed to exist when $P < 0.05$.

3. Results

3.1. Transition of B- to C-form DNA by Tan IIA in vitro

To illustrate the structure damage to duplex DNA upon binding with Tan IIA, the intrinsic CD spectra of DNA were performed. Cryptotanshinone, another extract of Tanshiones and an analogue of Tan IIA, was tested in parallel (structures shown in Fig. 1).

As shown in Fig. 2, the CD spectrum of free CT DNA exhibited a positive peak at 274 nm due to the base stacking and a negative band at 245 nm due to the helicity, which was the characteristic of DNA in the right-hand B-form [14]. With an increase in the concentration of Tan IIA, the decrease of the positive band and increase of the negative band suggested that Tan IIA induced certain conformational changes of DNA. Upon the binding, DNA double helix in solution became a more helical state belonging to the C-form DNA [15]. The same trend was found for cryptotanshinone/DNA complex under the same conditions, whereas the DNA conformational changes revealed much more weak than those induced by Tan IIA. It means although cryptotanshinone can also induce the B- to C-form conformational change, the torsion of DNA duplex is less than that caused by Tan IIA.

3.2. Effects of DNA conformational changes on RNAPII level in cells

To illustrate whether or not the DNA conformational changes induced by Tan IIA could inhibit transcription in living cells, degradation of RNAPII was measured in cells following Tan IIA, cryptotanshinone, and distamysin A treatments. Distamysin A, a classic minor groove binder, was brought in as a positive control. H22 cell line was applied because it was reported that Tan IIA showed significant antitumor properties against it [16,17].

As shown in Fig. 3, comparing with distamysin A, Tan IIA decreased the levels of RNAPII in a very similar dose-dependent manner. In contrast, no significant variation of RNAPII level was observed when the concentration of cryptotanshinone was varied incrementally from 2 to 24 μM. It demonstrated just like distamysin A, Tan IIA could induce RNAPII response and the response is related to the degree of the DNA conformational change. It worth noting that after 24 h exposure, the lowest concentration of Tan IIA at which we found RNAPII started to be downregulated was 4 μM.

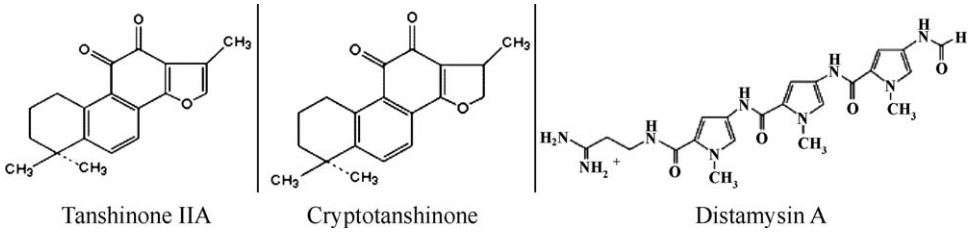

Fig. 1. Structures of tanshinone IIA, cryptotanshinone and distamysin A.

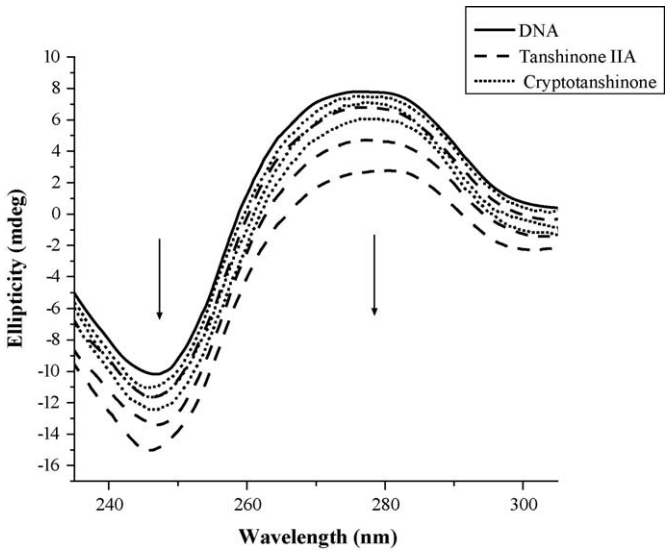

Fig. 2. Tan IIA caused B to C conformational change of duplex DNA larger than cryptotanshinone. Circular dichroism spectra of the titration of CT DNA with Tan IIA and cryptotanshinone in Tris–HCl (pH 7.0) were applied to understand the DNA conformational changes. Arrow indicates the increase of Tan IIA and cryptotanshinone concentration with 0, 10, 20, and 40 μM while the DNA concentration is 100 μM.

3.3. Phosphorylation and degradation of RNAPII in cells following Tan IIA treatment

Next, the phosphorylation of RNAPII in cells upon Tan IIA exposure was determined. After H22 cells were cultured with increasing concentrations of Tan IIA (0.2, 0.4, 4, 8, 12, 16, and 20 μM) for 48 h, cellular content of the unphosphorylated form (pol IIa) and phosphorylated form (pol IIo) was examined by western blot, respectively. As shown in Fig. 4, phosphorylation was monitored by observing a shift from pol IIa to pol IIo, which resulted in the increase of the level of pol IIo. This shift occurred at 0.4 μM, and the trend held till Tan IIA reached 4 μM. The amount of pol IIa began to decrease at the concentration of 0.4 μM of Tan IIA and progressively decreased within the dose frame of 0.4–20 μM. At the concentrations higher than 4 μM, the decrease of pol IIo was also detected. Thus, the dose-dependent RNAPII phosphorylation and degradation following Tan IIA treatment was testified.

3.4. Dynamics of RNAPII distribution along c-Myc gene in cells following Tan IIA treatment

Subsequently, we expanded the analyses to probe the dynamics of RNAPII distribution along a transcribed gene in cells following Tan IIA treatment. The chromatin binding site of RNAPII was mapped using ChIP and the DNA recovery levels were determined using Q-PCR.

The proto-oncogene c-Myc was chosen as a target since premature termination and pausing of RNAPII have been observed with this gene *in vivo* [9]. We examined the RNAPII levels bound to the P2 promotor fragment (A), exon fragment (B), and intron gene fragment (C). Since the reduction of RNAPII started at 24 h exposure of 4 μM of Tan IIA, and the lowest concentration at which Tan IIA may trigger the phosphorylation of RNAPII is 0.4 μM, we therefore broadened the dose frame to 0.2–4 μM and used 24 h incubation period to prevent significant protein loss due to degradation.

As shown in Fig. 5, the amount of RNAPII found at fragment A was markedly larger than that found at regions along the transcribed sequence. It is in agreement with the presence of a pause site at the P2 promoter [9]. In cells exposed to 0.2, 0.4, 2, and 4 μM of Tan IIA, RNAPII levels on all of the three fragments probed significantly decreased ($P < 0.01$ versus control). Dose-dependent RNAPII decrease along the whole length of transcribed gene template was detected. Interestingly, decrease of the bound RNAPII was obviously detected at the concentration of 0.2 μM, whereas under this concentration no phosphorylation was initiated by Tan IIA.

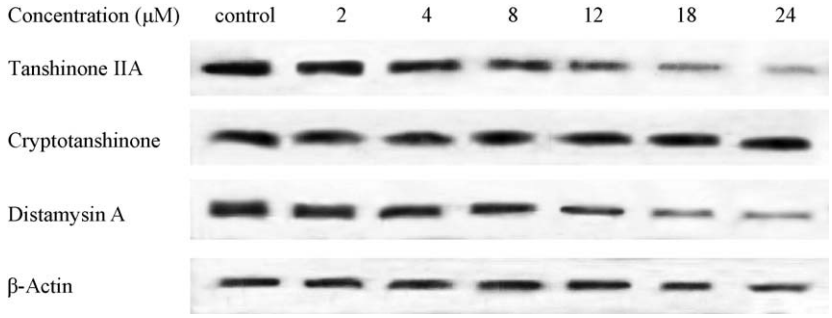

Fig. 3. Tan IIA and distamysin A, but not cryptotanshinone, caused concentration-dependence of RNAPII degradation. Western blot for the level of RNAPII in cells was performed. Total protein extracts from cells previously treated with drug vehicle (0.1% DMSO) alone as the control or 2, 4, 8, 12, 18, and 24 μM of each chemical for 24 h.

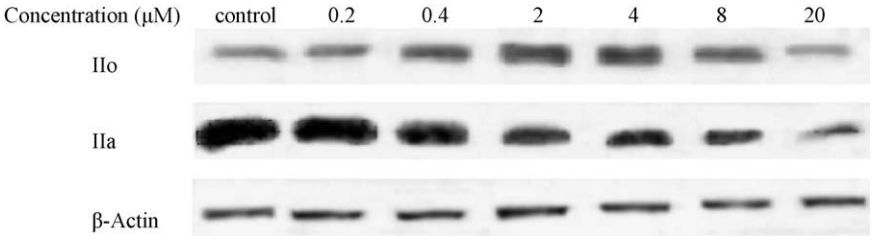

Fig. 4. Tan IIA induced phosphorylation and degradation of the level of RNAPII by western blot. IIo and IIa are the phosphorylaeted and unphosphorylated forms of the large subunit of RNAPII, respectively. Total protein extracts from cells previously treated with drug vehicle (0.1% DMSO) alone as the control or the indicated concentration of Tan IIA for 48 h.

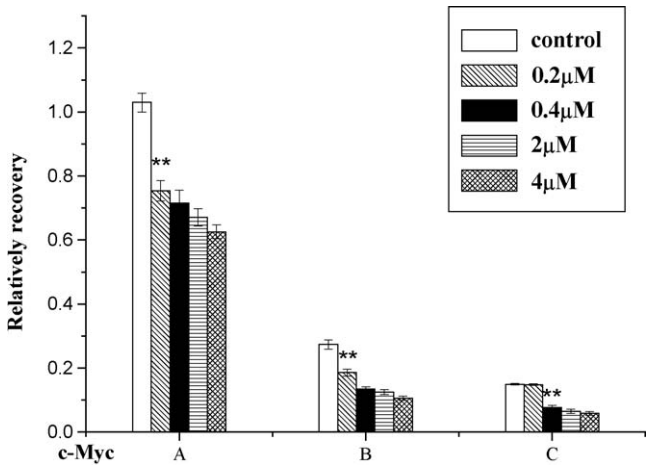

Fig. 5. Suppressive effects of Tan IIA on c-Myc gene binding patterns of RNAPII. RNAPII bound to fragments A (P2 promotor), B (exon region), and C (3′ end intron region) following drug vehicle (0.1% DMSO) alone or the indicated concentration of Tan IIA treated for 24 h are shown. DNA recovery is normalized relative to the fragment recovery of untreated cells. The values were obtained in three independent experiments performed in triplicate and were represented as means ± S.E. $^{**}P < 0.01$ versus control.

3.5. p53 activation and apoptosis induction by Tan IIA

It has been demonstrated that Tan IIA could activate p53 protein and induce apoptosis. We next investigated the relationship between p53 activation, apoptosis and RNAPII response. p53 activation and apoptosis upon Tan IIA exposure were tested within the dose frame that was revealed to be able to trigger RNAPII response by the aforementioned experiments. After H22 cells were cultured with 2.5, 4, 10, and 20 μM Tan IIA for 24 h, p53 activation was measured.

As shown in Fig. 6A, Tan IIA turned out to be an efficient trigger for p53 accumulation as well as an apoptosis inducer at the concentrations of 4 μM and upward. The level of p53 protein started to be upregulated at the same concentration that apoptosis occurred (4 μM), and p53 levels increased 5.9%, which was significantly higher than that observed in the control ($P < 0.01$). Interestingly, the RNAPII reduction also began at this concentration. A dose-dependent trend was observed for Tan IIA, where the stimulation of p53 reached 14.3% at a concentration of 20 μM. The concentration frame is consistent with both the occurrence of apoptosis and the degradation of RNAPII.

Next, we tested the apoptosis induction of Tan IIA in a p53 null cell K562. As shown in Fig. 6A, it took a higher dose of Tan IIA (10 μM) to achieve apoptosis induction in K562 than in H22. Moreover, the much weaker apoptotic induction was found for Tan IIA in K562 than H22 ($P < 0.01$).

Susequently, the apoptosis induction of Tan IIA and cryptotanshinone was investigated in parallel on H22 cells. Fig. 6B–D showed after 24 h exposure of 8 μM Tan IIA, 26.8% H22 cells ($P < 0.01$ versus control and cryptotanshinone group) exhibited early phase of apoptosis (green cells which nucleus present pyknosis). In the case of cryptotanshinone, only 2.5% cells ($P > 0.05$ versus control) were apoptotic under the same conditions.

3.6. Degradation of RNAPII and apoptosis induction by Tan IIA in vivo

In order to test whether or not Tan IIA induces degradation of RNAPII and apoptosis by RNAPII *in vivo*, ascitic-type hepatic carcinoma H22 mice model was set up. After i.p. injected with 20 and 40 mg/kg body weight of Tan IIA for 10 days, respectively, content of RNAPII in ascitic cells was examined by western blot and tumor cell apoptosis was measured by the TUNEL method. As shown in Fig. 7A, in cells from 10 mice injected with 40 mg/kg body weight Tan IIA, the amount of RNAPII was significant diminished

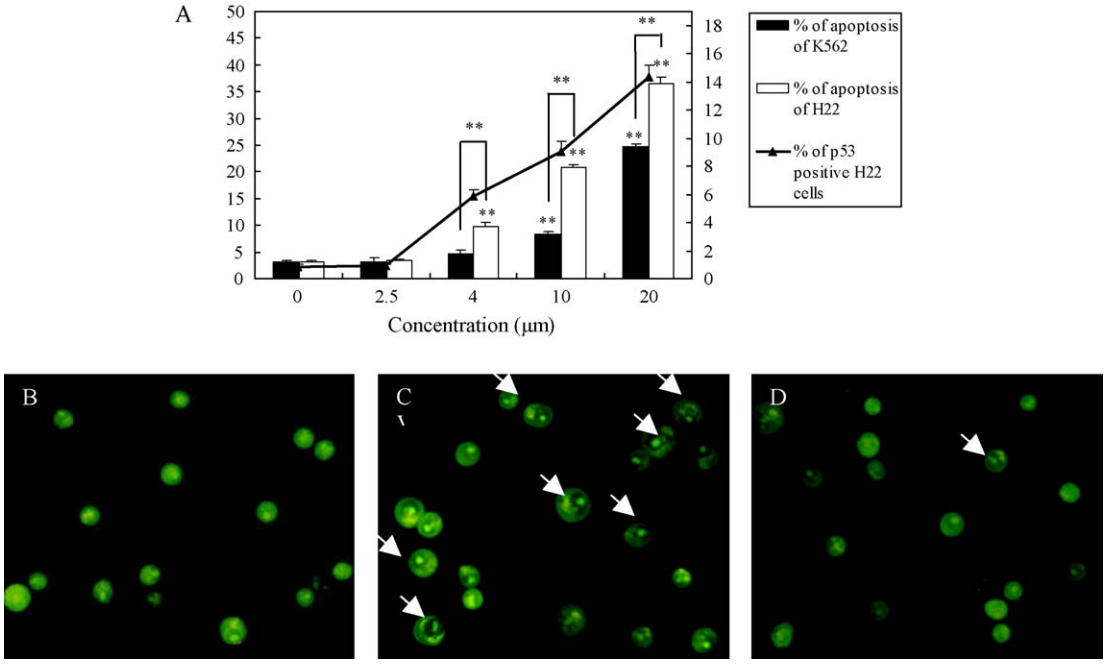

Fig. 6. Tan IIA induced activation of p53 and correlative apoptosis. (A) H22 and K562 cells were seeded into 6-well plates and treated with drug vehicle (0.1% DMSO) alone or different concentrations of Tan IIA (2.5, 4, 10, and 20 μM, respectively) for 24 h, respectively. Cells were then fixed and stained with an anti-p53 antibody (DO-1) and PI staining for flow cytometry analysis, respectively. At least 10,000 events were counted for each sample. The graphic represents a quantification of cells activated. The means and S.E. for three independent experiments are shown (significance is indicated by asterisks: $^{**}P < 0.01$). (B–D) LIVE/DEAD/APOPTOSIS two-color cell viability experiment was used to measure tumor cell apoptosis induced by Tan IIA and cryptotanshinone, respectively. (B) Untreated H22 cells (live, negative control), (C) cells exposed to 8 μM Tan IIA for 24 h (cells indicated by arrows are early apoptotic cells), and (D) cells exposed to 8 μM cryptotanshinone for 24 h (cells indicated by arrows are early apoptotic cells).

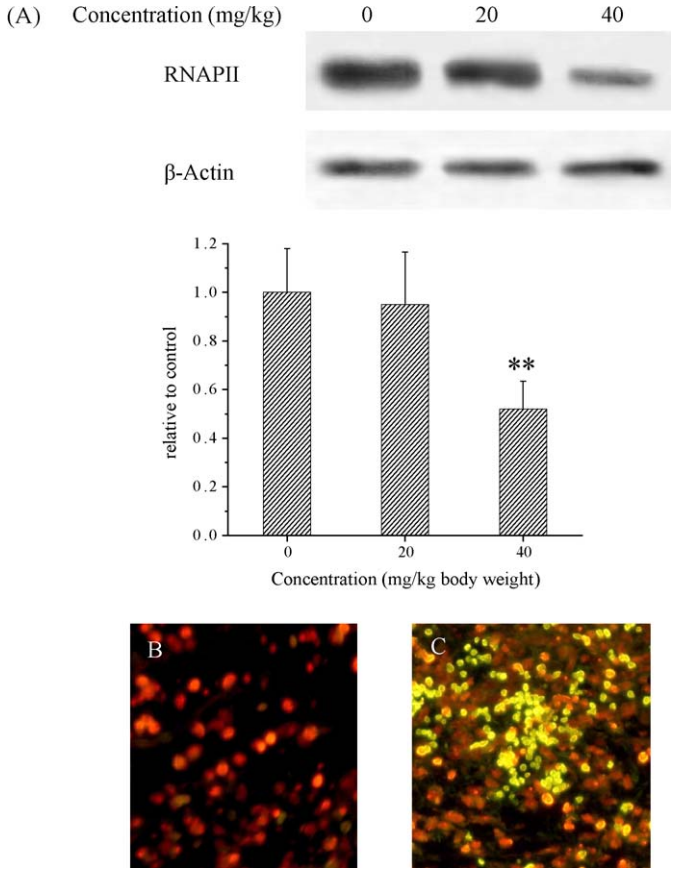

Fig. 7. Tan IIA induced degradation of RNAPII and apoptosis *in vivo*. Ascitic-type hepatic carcinoma H22 mice model was set up, and administered with different concentrations of Tan IIA (0, 20, and 40 mg/kg body weight, $n = 10$, respectively) for 10 days. (A) Content of RNAPII in ascitic tumor cell was examined by western blot, and the content of RNAPII in the group injected with 40 mg/kg Tan IIA was obvious diminished comparing with the control (**$P < 0.01$), while that with 20 mg/kg was close to the control. (B) Tumor cell apoptosis was measured by the TUNEL method. Photomicrographs of TUNEL-stained cell from a control mouse and (C) a mouse treated with Tan IIA (40 mg/kg), which showed increased positive nuclear staining (green). (For interpretation of the references to color in this figure legend, the reader is referred to the web version of the article.)

comparing with the 10 control mice, while that from mice treated with 20 mg/kg body weight was close to the control. In the same way, TUNEL assay demonstrated a relatively low level of apoptosis within tumor cells from the 10 control mice (median number of TUNEL-positive cells per 200× microscopic field = 3.1 ± 1.4, shown in Fig. 7B). In contrast, cells from the mice treated with Tan IIA (40 mg/kg body weight) showed an about twice increase in the median number of apoptotic cells per field (6.7 ± 1.6, $P < 0.01$, Fig. 7C) compared with the control mice. In the mice receiving Tan IIA at the dose of 20 mg/kg body weight, no significant increase was found (2.7 ± 0.6, $P > 0.05$, figure not shown).

4. Discussion

Although the anticancer activity of Tan IIA has been identified in mouse hepatic carcinoma, breast cancer cell line and so on, Tan IIA shows no general toxicity at certain doses [18,19]. It promotes us to unveil the underlying antitumor molecular parmarcology of Tan IIA. Based on our surprising previous finding that Tan IIA is a groove binder, we firstly illustrated the B- to C-form DNA conformational change induced by Tan IIA in the present study. Comparing with DNA intercalators, the DNA structure change induced by Tan IIA is much minor [20]. On one hand, it may to some extent explain that Tan IIA generally exhibits no toxicity. On the other hand, it promotes us to investigate if transcription machinery is involved in the antitumor pharmacology of Tan IIA because it has been proved for different DNA-groove-binding drugs that they could arrest transcription by RNAPII by altering the conformation of transcribed DNA. As such, we compared the cellular RNAPII response upon Tan IIA and distamysin A exposure. Although Tan IIA is structurally distinct from distamysin A, it nevertheless shares the minor groove and AT-rich binding site characteristic of distamysin A. Frequently, sites that arrest RNAPII are often stretches of AT base pairs. As expected, results of western blot showed the cellular RNAPII degradation upon exposure to Tan IIA is very similar to that exposed to distamysin A. It demonstrated that Tan IIA has the overall same effects on RNAPII with distamysin A. We next investigated if the RNAPII response associates directly with the DNA conformational change upon Tan IIA binding. To this end, we examined whether the related effects of Tan IIA and cryptotanshinone on the cellular RNAPII level are consistent with their related DNA conformational damage. Although cryptotanshinone is a very analog of Tan IIA, it induces DNA conformational change much less weakly than Tan IIA. Comparable, cryptotanshinone cannot reduce RNAPII as much as Tan IIA. Finally, cryptotanshinone cannot induce apoptosis as significant as Tan IIA can, which is in agreement with the previous findings [21]. It demonstrated RNAPII response is due to the DNA conformational change and correlates with the degree. Collectively, we have observed that DNA-conformational-damage-dependent RNAPII response upon groove binding is the molecular basis of antitumor property of Tan IIA.

Subsequently, we investigated the mechanism of RNAPII reduction by Tan IIA. Because RNAPII could be phosphorylated in the initial steps of DNA damage and accounts for the degradation of RNAPII [22], we measured the cellular level of pol IIa and pol IIo form of the polymerase, respectively. The phosphorylation was found by observing a shift from IIa to IIo. The phosphorylation occurred at 0.4 μM of Tan IIA exposure, where the amount of IIa dropped and IIo increased. In the dose range of 0.4–4 μM, the phosphorylation continued. When the dose reached 4 μM, the promising degradation of RNAPII was found that both IIo and IIa were decreased. To deeply understand how RNAPII works upon Tan IIA exposure, we investigated the dynamics of RNAPII distribution along a transcribed gene in cells following Tan IIA treatment. Except for dose-dependent RNAPII decrease along the gene, we surprisingly found that the inhibition of RNAPII binding to gene occurred at a concentration as low as 0.2 μM, at which its phosphoralytaion and reduction had not started yet. By far, we concluded that RNAPII is first of all inhibited to bind with transcribed gene by Tan IIA due to the double helix structure changes. Consequently, the inhibition triggers the phosphorylation of RNAPII, in turn results in its degradation. It may be the basis of apoptosis induction because the degradation of RNAPII is a general response to stalled or arrested elongation complex [23], which can strongly trigger p53 activation then apoptosis.

The p53 activation and apoptosis assays on H22 cells and p53 deficient K562 cells confirmed our hypothesis. On H22 cells, p53 started to be upregualted after the full phosphorylation of RNAPII and exactly at the same concentration where the RNAPII level stared to be downregulated (4 μM). Apoptosis began also at this concentration. The dose-dependent p53 activation was found in the dose range of 4–20 μM of Tan IIA treatment, so was the apoptosis. The dose frame consists with that Tan IIA could induce RNAPII degradation. It strongly suggested that Tan IIA induces p53 mediated apoptosis by RNAPII. Additionally, the significant less apoptosis induction of Tan IIA was found in the case of K562 cells under the same conditions. It further demonstrated that p53 plays an important role in Tan IIA inducing apoptosis. Because p53 is not the only downstream factor of RNAPII, Tan IIA may still exhibit

some apoptosis inducing ability on K562. Wang et al. demonstrated that caspase 3 is one of the targets of Tan IIA [2]. Because caspase 3 is the downstream effector of p53, the mechanism revealed in this report is more deeply than the previous one. Another significant finding is that during the relatively lower and wider dose frame of Tan IIA exposure (0.4–4 μM) where RNAPII phosphorylation was continued, neither p53 activation nor apoptosis occurred. On one hand, it is in agreement with the knowledge that only after RNAPII is fully phosphrylated does transcription block trigger p53 activation [24]. On the other hand, this result could be interpreted as that Tan IIA shows no general toxicity at certain doses. At the dose range of 0.2–4 μM, apoptosis does not occur even though the inhibition of RNAPII binding to transcribed gene and phosporylation can be found. In some previous reports, the doses that Tan IIA could induce apoptosis are ranging from 2 to 40 μM [25–27], while the safe doses (free of cytotoxicity) for Tan IIA are ranging from 0.01 to 10 μM [18,28]. Although the doses vary so much due to the different experiment conditions and different cell lines, it still hints that Tan IIA does not possess cytotoxicity under relatively lower doses. Within this dose window it may be used as anti-inflammatory or antioxidant agent safely. Our findings may give a molecular insight for this property.

Next, the *in vivo* anticancer activity of Tan IIA was investigated. The dose-dependent RNAPII reduction and apoptosis were found in xenotransplant animals. Tan IIA did not show apoptosis inducing ability until it significantly downregualted RNAPII at the dose of 40 mg/kg body weight. Tan IIA induced apoptosis by RNAPII was identified *in vivo*.

In summary, the molecular antitumor pharmacology of Tan IIA was illustrated. Under relative lower doses of Tan IIA exposure, structure changing of duplex DNA results in the inhibition of RNAPII binding to transcribed gene, which leads to the phosphorylation of RNAPII. As the dose increasing, RNAPII subjects full phophorylation and degradation, which triggers p53 activation and then apoptosis. The antitumor ability of Tan IIA is dependent on RNAPII degradation. Additionally, the results in the present report strongly demand the need to identify the dose frame that Tan IIA could be safe, or could induce apoptosis in normal and/or other cancer cells.

Acknowledgment

This work was supported by the National Natural Science Foundation of China (30772622).

References

[1] Ryu SY, Lee CO, Choi SU. In vitro cytotoxicity of tanshinones from *Salvia miltiorrhiza*. Planta Med 1997;63:339–42.
[2] Wang X, Wei Y, Yuan S, Liu G, Lu Y, Zhang J, et al. Potential anticancer activity of tanshinone IIA against human breast cancer. Int J Cancer 2005;116:799–807.
[3] Wu WL, Chang WL, Chen CF. Cytotoxic activities of tanshinones against human carcinoma cell lines. Am J Chin Med Am J Chin Med 1991;19:207–16.
[4] Wang X, Morris-Natschke SL, Lee KH. New developments in the chemistry and biology of the bioactive constituents of Tanshen. Med Res Rev 2007;27:133–48.
[5] Zhang Z, Zhang J, Jin L, Song T, Wu G, Gao J. Tanshinone IIA interacts with DNA by minor groove-binding. Biol Pharm Bull 2008;31:2342–5.
[6] Scicchitano DA, Olesnicky EC, Dimitri A. Transcription and DNA adducts: what happens when the message gets cut off? DNA Repair 2004;3:1537–48.
[7] Straney DC, Crothers DM. Effect of drug–DNA interactions upon transcription initiate ion at the lac promoter. Biochemistry 1987;26:1987–95.
[8] Mote Jr J, Ghanouni P, Reines D. A DNA minor groove-binding ligand both potentiates and arrests transcription by RNA polymerase II. J Mol Biol 1994;236:725–37.
[9] Khobta A, Ferri F, Lotito L, Montecucco A, Rossi R, Capranico G. Early effects of topoisomerase I inhibition on RNA polymerase II along transcribed genes in human cells. J Mol Biol 2006;357:127–38.
[10] Reitsema T, Klokov D, Banáth JP, Olive PL. DNA-PK is responsible for enhanced phosphorylation of histone H2AX under hypertonic conditions. DNA Repair (Amst) 2005;4:1172–81.
[11] Gaiddon C, Jeannequin P, Bischoff P, Pfeffer M, Sirlin C, Loeffler JP. Ruthenium (II)-derived organometallic compounds induce cytostatic and cytotoxic effects on mammalian cancer cell lines through p53-dependent and p53-independent mechanisms. J Pharmacol Exp Ther 2005;315:1403–11.
[12] Wang L, Zhou GB, Liu P, Song JH, Liang Y, Yan XJ, et al. Dissection of mechanisms of Chinese medicinal formula Realgar-*Indigo naturalis* as an effective treatment for promyelocytic leukaemia. Proc Natl Acad Sci USA 2008; 105:4826–31.
[13] Gavrieli Y, Sherman Y, Ben-Sasson SA. Identification of programmed cell death in situ via specific labeling of nuclear DNA fragmentation. J Cell Biol 1992;119:493–501.
[14] Jiang X, Shang L, Wang Z, Dong S. Spectrometric and voltammetric investigation of interaction of neutral red with calf thymus DNA: pH effect. Biophys Chem 2005;118:42–50.
[15] Zuidam NJ, Barenholz Y, Minsky A. Chiral DNA packaging in DNA-cationic liposome assemblies. FEBS Lett 1999;457:419–22.
[16] Wang X, Yuan S, Wang C. A preliminary study of the anti-cancer effect of tanshinone on hepatic carcinoma and its mechanism of action in mice. Zhonghua Zhong Liu Za Zhi 1996;18:412–4.
[17] Yuan SL, Wei YQ, Wang XJ, Xiao F, Li SF, Zhang J. Growth inhibition and apoptosis induction of tanshinone IIA on human hepatocellular carcinoma cells. World J Gastroenterol 2004;10:2024–8.
[18] Liu Y, Wang X, Liu Y. Protective effects of tanshinone IIA on injured primary cultured rat hepatocytes induced by CCl4. Zhong Yao Cai 2003;26:415–7.
[19] Liu Chen H, Jiang Y. Protective effect of tanshinone IIA on acute hepatic injury in mice. Zhong Yao Cai 2001;24:588–9.
[20] Nelson SM, Ferguson LR, Denny WA. Non-covalent ligand/DNA interactions: minor groove binding agents. Mutat Res 2007;623:24–40.
[21] Lee WYW, Chiu LCM, Yeung JHK. Cytotoxicity of major tanshinones isolated from Danshen (*Salvia miltiorrhiza*) on HepG2 cells in relation to glutathione perturbation. Food Chem Toxicol 2008;46:328–38.
[22] Zhang Z, Wang Y, Song T, Gao J, Wu G, Zhang J, et al. DNA double helix unwinding triggers transcription block-dependent apoptosis: a semiquantitative probe of the response of ATM, RNAPII, and p53 to two DNA intercalators. Chem Res Toxicol 2009;22:483–91.
[23] Luo Z, Zheng J, Lu Y, Bregman DB. Ultraviolet radiation alters the phosphorylation of RNA polymerase II large subunit and accelerates its proteasome-dependent degradation. Mutat Res 2001;486:259–74.
[24] Ljungman M, Lane DP. Transcription—guarding the genome by sensing DNA damage. Nat Rev Cancer 2004;4:727–35.
[25] Hu H, Zhang Y, Huang F, Deng H. Inhibition of proliferation and induction of apoptosis by tanshinone IIA in NCI-H460 cell. Zhong Yao Cai 2005;28:301–4.
[26] Zhou L, Chan WK, Xu N, Xiao K, Luo H, Luo KQ, et al. Tanshinone IIA, an isolated compound from *Salvia miltiorrhiza Bunge*, induces apoptosis in HeLa cells through mitotic arrest. Life Sci 2008;83:394–403.
[27] Wang X, Xie YX, Shan BE. Effects of tanshinone IIA on proliferation and apoptosis of the human gastric cancer cell line BGC-823. Carcinogenesis Teratogenesis & Mutagenesis 2008;20:56–9.
[28] Yuan S, Wei Y, Wang W, Xiao F, Li S, Zhang J. Growth inhibition and apoptosis induction of tanshinone II-A on human hepatocellular carcinoma cells. World J Gastroenterol 2004;10:2024–8.